

ROCKET-BORNE SERVO-SYSTEM

by

W.S. BLACK

A B S T R A C T

This paper reports on the design of the fine alignment servo-system developed for solar spectroscopy by the Natural Plasma Group at Culham. Graphical methods are given for finding the transfer function of the servo and methods for producing a stable system are discussed.

U.K.A.E.A. Research Group,
Culham Laboratory,
Nr. Abingdon,
Berks.

August, 1965 (C/18 MEA)

C O N T E N T S

	<u>Page</u>
1. INTRODUCTION	1
2. FREQUENCY RESPONSE METHOD OF DESIGN	2
3. GRAPHICAL METHODS	3
4. STABILISATION TECHNIQUES	3
5. TRANSFER FUNCTION OF THE SERVO-MOTOR	5
6. SERVO SYSTEM	6
7. CONCLUSIONS	8
8. ACKNOWLEDGMENTS	8
9. REFERENCES	8

1. INTRODUCTION

Experiments being undertaken by Culham Laboratory to obtain the spectrum of the solar corona and chromosphere in the far ultra-violet region 500-3000Å⁽¹⁾, require a normal incidence spectrograph to be flown in a Skylark sounding rocket. In order to achieve this, the normal incidence experiment requires a pointing accuracy of one minute of arc to allow alignment close to the edge of the solar disc. This requirement has been met by the fine alignment servo system to be described.

The servo system controls a platform carrying the main mirror which images the solar disc so that the limb of the sun is tangential to the spectrograph slit. Mounted on the same platform is an auxillary mirror which images the solar disc onto a split field photo-voltaic error detector and provides the feedback loop for the servo. The error signals are fed to servo-motors which tilt the mirror platform about two mutually perpendicular axes and thus maintain alignment⁽²⁾.

In Fig.1, one axis of the system is shown. The signal from the error detector is fed into the error detector unit which contains a d.c. pre-amp, the stabilising networks, and a 400 c/s modulator. The output from this unit is therefore a 400 c/s carrier modulated by the error signal and is thus suitable to drive the a.c. servo-motor. The modulated carrier signal is fed via the target eye relay to the servo-amplifiers which, besides amplifying the signal, also produces the necessary 90° phase difference required between control and reference windings of the motor.

During the boost phase and acquisition by the rocket attitude control system, the fine solar alignment system is locked electrically by a.c. pick-offs which are fixed to the mirror cam shaft. The characteristics of the pick-offs are such that if the rotor of the unit is displaced angularly from its null point, then a 400 c/s signal is produced which has a magnitude proportional to the angular displacement of the rotor and its phase is reversed on either side of the null point. Hence, if the pick-offs are switched into the servo loop they will drive the motors until the null point is reached, thus 'locking' the mirror platform. The mirror is held in this position until the payload comes into the field of view of the target eye. The output from the target eye is processed in the target eye unit which operates a relay, and the servo loop is then controlled by the error detector, thus allowing the servo to track during the experimental flight time.

The analysis of such a feedback control system can be carried out in either the time or frequency domain. In the time domain, the performance criteria and specifications are

obtained from the differential equation of the system. Having obtained the solution, three basic input functions - step displacement, velocity, and acceleration - are then applied so that the performance of the system can be evaluated in terms of transient and steady state response.

In the frequency domain all that is required is the response of the system to a sinusoidal input at varying frequencies. This method is mainly a graphical approach to the design of a servo system and, as such, gives a quicker insight into the problems associated with the system design. This is the method here adopted and described in following sections of the paper.

2. FREQUENCY RESPONSE METHOD OF DESIGN

The essential feature of the frequency response method is that the description of the system is given in terms of its response to a sinusoidally varying input signal. If the system is linear, then the gain of the system can be represented by a magnitude and a phase angle. Thus, if $G(j\omega)$ is the open loop gain then the transfer function is $G(j\omega) = |G| \angle \phi$ where $|G|$ is the magnitude and $\angle \phi$ the phase angle at different frequencies. The frequency response method therefore entails finding the response of each element in the servo system so that the overall transfer function meets the required specifications when the servo loop is closed.

The transfer function of a closed loop unity feed-back system under steady state conditions is given by $M \angle \phi_m = \frac{G(j\omega)}{1 + G(j\omega)}$ where M is the closed loop gain and G the open loop gain. Since the value of M depends on G , then suitable design of the open loop gain will produce a stable system. The performance of the servo system in the frequency domain is usually specified by the following -

Bandwidth	-	This is the frequency at which the closed loop response has fallen 3db from its zero frequency gain.
Resonance Peak M_p	-	The maximum value which the closed loop gain M attains.
Resonant Frequency ω_p	-	The frequency at which the resonance peak occurs.
Gain Margin	-	The increase in gain that can be tolerated before the system becomes unstable.
Phase Margin	-	The increase in phase lag that can be allowed before instability occurs.
Velocity Error	-	This is the error by which the output lags the input when the servo is tracking at a constant velocity. It is not an error in velocity but an error in displacement due to a velocity input.

(Fig.13)

3. GRAPHICAL METHODS

There are various methods for plotting the transfer function $G(j\omega)$, and the following are particularly useful in the analysis and design of feedback control systems.

Polar Plot This is a plot of magnitude versus phase shift on polar co-ordinates as the frequency is varied.

Bode Plot A plot of gain in db and phase shift in degrees against frequency.

Gain/Phase Shift The gain in db is plotted against phase with frequency as the varying parameter.

The polar plot is used for determining instability by use of the Nyquist stability criterion which states that for a stable closed loop system the open loop gain must be less than unity when the phase lag in the system reaches 180° . The degree of stability is indicated by how far the gain is below unity at a 180° phase shift (Fig.2).

The Bode plot has the advantage that the product factors in the expression $G(j\omega)$ become additive since logarithms are used. The plots are also easy to construct, and it is possible to represent the exact function by straight line asymptotes. This is shown in Appendix A and Figs.3, 5 and 6.

In order to evaluate the closed loop response, the open loop gain and phase (Fig.4) can be plotted on a Nichols Chart⁽³⁾. On this chart constant closed loop contours have been superimposed on open loop co-ordinates, thus the data from the Bode plot can be constructed on the chart and the closed loop response determined by inspection.

4. STABILISATION TECHNIQUES

A high performance system implies a high open loop gain and, as such, usually leads to instability. It is generally impossible to satisfy all the performance specifications for steady state response, transient response, and stability with the basic elements, which must, therefore, be provided by some other means. The instability with the loop closed is due to the phase angle between input and output lagging 180° , whilst the open loop gain is greater than unity. A network which has the ability to reduce the phase lag is the Phase Advance network (Fig.7).

Phase Advance

The transfer function of this network is given by -

$$\left(\frac{V_o}{V_i}\right)_{j\omega} = \frac{1}{a} \frac{1 + j\omega T}{1 + j\omega \frac{T}{a}} \quad \text{where} \quad a = \frac{R_1 + R_2}{R^2} \quad a > 1$$

$$T = \frac{R_1 R_2}{R_1 + R_2} C$$

A Bode plot of this function can be drawn easily by plotting $(1 + j\omega T)^1$ and $(1 + j\omega T)^{-1}$. This shows two break frequencies at $\omega_1 = 1/aT$ and $\omega_2 = 1/T$ and if the two functions are added the resultant curve is obtained. The plot also shows the frequency at which the phase angle of the network is a maximum. Thus, if the network is designed to produce this maximum phase angle at the point where the phase lag in the servo becomes critical, the phase lag is reduced and the system can be made stable.

The values in the table below give the gain and phase relations for a phase advance network -

ωT	0	0.2	0.5	0.8	1	2	3.16	5	10	15
Gain	1	1.02	1.12	1.27	1.41	2.19	3.16	4.56	7.11	8.35
Phase	0	10.1	23.7	34.1	39.3	52.1	54.9	52.1	39.3	29.9

Phase Lag

If the servo is expected to operate at very low frequencies, or track at a constant velocity, then by allowing the gain of the system to increase at the lower frequencies the steady state, or tracking error, can be made very small. A circuit which achieves this is the phase lag network, and its transfer function is given by -

$$\left(\frac{V_2}{V_1}\right)_{j\omega} = \frac{1 + j\omega bT}{1 + j\omega T} \quad b < 1$$

$$b = \frac{R_2}{R_1 + R_2} \quad bT = CR_2$$

A Bode plot again shows two break frequencies and a maximum phase lag. However, the design of the network does not rely on this maximum phase lag but on the attenuation of the network at the higher frequencies. This increase in gain at the lower frequencies can reduce the error by as much as $1/b$. Refer to Fig.8.

A combination of lead and lag networks can be used giving a transfer function -

$$\left(\frac{V_o}{V_i} \right)_{j\omega} = \frac{(1 + j\omega a T_1)}{(1 + j\omega T_1)} \frac{(1 + j\omega b T_2)}{(1 + j\omega T_2)}$$

phase lead phase lag

where $a > 1$ $b < 1$ and $ab = 1$, i.e. once the value of b is determined then a is the reciprocal. Refer to Fig.9.

5. TRANSFER FUNCTION OF THE SERVO-MOTOR

The major item in any servo system is the controller which drives the load. In the present system the controller is a 2-phase 400 c/s induction servo-motor. In order to obtain the transfer function of the motor some approximations are necessary. The first approximation is that the torque/speed characteristic of the motor are linear (Fig.10). By careful design, the manufacturers of small, high performance servo-motors approach such a characteristic. The ideal curve is further approached due to the fact that most servo systems seldom operate at high speeds but search around a null point. From the torque/speed characteristic the viscous friction (inherent damping) of the motor can be computed. In practice, the value found is valid up to half no-load speed.

When finding the transfer function of the motor, any inertia reflected from the load must be taken into account. The present system has a step-down gear ratio of 10^4 , thus the load inertia is assumed to be negligible. The transfer function of the motor is derived in Appendix B.

From a plot of the motor transfer function -

$$\left(\frac{\theta_o}{V} \right)_{j\omega} = \frac{K_m}{j\omega(1 + j\omega T_m)} \quad \text{where } T_m = \text{mechanical time constant}$$

the phase characteristics start from 90° lagging, and approach 180° lagging, but cannot exceed 180° at any frequency. This implies that if there is no other frequency dependent element in the servo then the gain could be increased indefinitely without instability occurring. However, experimentally this is not supported and a more complex transfer function is required

$$\left(\frac{\theta_o}{V} \right)_{j\omega} = \frac{K_m}{j\omega(1 + j\omega T_m)(1 + j\omega T_2)}$$

where T_2 corresponds to the electrical time constant L/R of the motor. Fortunately, L/R does not appear at the lower frequencies and provided the bandwidth of the servo system is limited to a much lower frequency than $\omega_2 = 1/T_2$ then the effect of L/R is small.

Other effects which produce instability in a high performance servo system are slot effect, bearing friction and backlash.

Slot effect is the minimum voltage applied to the control phase of the motor which will cause it to rotate and represents a basic error in the system. Likewise, bearing friction and backlash will degrade system performance.

6. SERVO SYSTEM

The fine alignment system is required to maintain the position of the solar image to better than 1 arc mm. As this is the maximum allowable error for the whole experiment the error allowed for the servo was limited to 10 arc secs.

The tracking velocity during flight was not expected to exceed $1^{\circ}/\text{sec.}$, therefore the gain of the system has to be at least $K_v = 360 \text{ sec}^{-1}$. The bandwidth of the fine alignment system must be greater than that of the rocket stabilising system, and a bandwidth of 25 c/s was aimed at. Stability was of prime importance as there would be an unavoidable increase in error detector sensitivity due to reduced atmospheric absorption at higher altitudes.

A plot of the motor transfer function showed that with the required gain the system would be oscillatory and would require stabilisation. This instability is due not only to the motor phase lag, but also to the phase lag introduced by the sampling frequency which 'chops' the d.c. error signal at 400 c/s to drive the servo motors. From examination of the plot, the data required for the phase advance network was obtained and the network designed to give adequate phase and gain margins. Having obtained a stable system, the introduction of a phase lag network can be considered to improve the steady state error. When designing the phase lag or integral network care must be taken to avoid too much reduction of the original phase margin. If the time constant of the network is too small, the phase lag introduced by the network can cancel the effect of the phase advance and the system can become oscillatory. On the other hand, too large a time constant will produce a sluggish system with a poor transient response. A figure to be aimed at is 10° lag introduction by the network. This would make $\omega = 1/bT$ about one fifth the gain crossover frequency of the servo.

The transfer function of the complete servo is found by multiplying the transfer functions of the separate elements in the block diagram. Thus, we have

$$\left(\frac{\theta_0}{\theta_1} \right)_{j\omega} = \frac{K_v}{j\omega(1 + j\omega T_m)}$$

where $K_v = K_e K_a K_m K_n$

K_e = error detector sensitivity

K_a = amp. gain

K_m = motor gain constant

K_n = gear ratio

The value of K_v when evaluated will give the steady state velocity gain constant, which is defined as the ratio of output velocity to the steady state error, i.e.

$$K_v = \frac{w_0}{\text{ESS}} \text{ sec}^{-1}$$

From the above definition it can be seen that the gain of the system required can be found if the allowable error in the system is specified along with maximum tracking speed. A plot of the above transfer function K_v in db's and phase angle, against frequency will show what adjustments have to be made to ensure stability when the servo loop is closed. This is shown in Figs.11 and 12.

An initial plot of the function

$$\left(\frac{\theta_o}{\theta_i} \right)_{jw} = \frac{360}{jw(1 + jw 0.012)}$$

gave a slope of -20 db/decade until the break frequency $w = 1/T_m = 83.4$ rad/sec. The slope then continued at -40 db/decade and crossed the zero db line at 150 rad/sec, with a phase lag of 153° . The phase advance network was designed to produce maximum phase lead at this frequency. This gave a first break frequency for the network of $w_3 = 90$ rad/sec, i.e.

$$w_3 = 1/aT = 90 \text{ rad/sec} \text{ where } a \doteq 10$$

$$\therefore T = 1/900 = 0.0011 \text{ secs.}$$

The transfer function is therefore given as

$$\left(\frac{V_o}{V_i} \right)_{jw} = \frac{(1 + jw 0.011)}{(1 + jw 0.0011)}$$

The phase lag network was designed to have its second break frequency at one fifth of the crossover frequency

$$w_2 = w_c/5 = 30 \text{ rad/sec}$$

i.e.

$$bT = 1/30$$

$$b \doteq 0.1$$

$$T = 1/3 = 0.33 \text{ secs}$$

The transfer function is therefore

$$\left(\frac{V_o}{V_i} \right)_{j\omega} = \frac{(1 + j\omega 0.033)}{(1 + j\omega 0.33)}$$

Thus

$$\left(\frac{\theta_o}{\theta_i} \right)_{j\omega} = \frac{360 (1 + j\omega 0.033) (1 + j\omega 0.011)}{j\omega (1 + j\omega 0.012) (1 + j\omega 0.033) (1 + j\omega 0.0011)}$$

The gain of the system was increased to compensate for the loss in the networks giving a velocity gain constant of 3600, thus the theoretical tracking error is reduced to 1 arc-sec.

The closed loop performance was then checked by a transfer function analyser. The system required little modification to the original design, and the final figures gave a bandwidth of 22 c/s with phase and gain margins of 50° and 10 db respectively.

7. CONCLUSIONS

This approach to the design of the fine alignment system, whilst not exhaustive, provides a reasonably accurate method of tackling the problem of servo design.

Two rockets containing the fine alignment system have been fired from the Woomera rocket range in Australia and telemetry records show that the system retained control over a flight period of four minutes, with tracking errors not exceeding 12 arc-secs peak to peak.

8. ACKNOWLEDGMENTS

To Mr. D.B. Shenton who designed the mirror platform, and Mr. J.G. Firth for his assistance in building and testing the servo system.

9. REFERENCES

1. BLACK, W.S., BOOKER, D., BURTON, W.M., JONES, B.B., SHENTON, D.B. and WILSON, R. Solar spectroscopy in the extreme ultraviolet using stabilized Skylark rockets. Nature, vol.206, no.4985, 15 May 1965. pp.654-658.
2. BLACK, W.S. and SHENTON, D.B. Fine solar alignment system for operation in stabilized vehicles. I.F.A.C. Symposium on Automatic Control in the Peaceful Uses of Space, Stavanger, June 1965.
3. JAMES, H.M., NICHOLLS, N.B. and PHILLIPS, R.S., eds. Theory of servomechanisms. New York, McGraw Hill, 1947.

APPENDIX A

Common functions in servo design are $(j\omega)^{\pm n}$ and $(1 + j\omega T)^{\pm 1}$. The magnitude of $(j\omega)^{\pm n}$ in db is given by

$$20 \log (j\omega)^{\pm n} = \pm 20n \log \omega$$

The slope of the lines is given by

$$\frac{d \ 20 \log (j\omega)^{\pm n}}{d \log \omega} = \pm 20n \text{ db}$$

i.e. the slope changes at 20 db per decade of frequency and the phase shift of $(j\omega)^{\pm n}$ is $\pm n$ 90 degrees. The plot of the above is shown in Fig.5.

The magnitude of $(1 + j\omega T)^{\pm 1}$ is given by

$$20 \log |G j\omega| = \pm 20 \log \sqrt{1 + \omega^2 T^2}$$

The approximations for the plot of the function at low frequencies, i.e. $\omega T \ll 1$, is given by

$$20 \log |G j\omega| = 20 \log 1 = 0 \text{ db} \quad \dots (1)$$

and at very high frequencies, i.e. $\omega T \gg 1$

$$\begin{aligned} 20 \log |G j\omega| &= 20 \log \omega T \\ &= 20 \log \omega + 20 \log T \end{aligned} \quad \dots (2)$$

This represents a straight line with a slope of 20 db per decade of frequency.

The intersection of the low and high frequency asymptotes is found by equating, i.e.

$$20 \log \omega T = 0 \text{ db}$$

from which $\omega T = 1$.

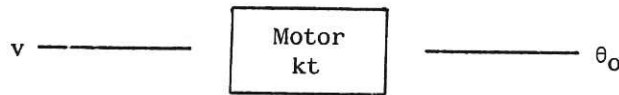
The value of $\omega = 1/T$ is called the break, or corner, frequency of the plot, and the phase angle at this frequency is $\phi = \tan^{-1} \omega T = 45^\circ$. The plots are shown in Fig.6.

Although the actual curve of the magnitude plot is smooth, the table shows that the errors introduced by the straight line approximation are small.

ωT	ϕ degrees	$ 1 + j\omega T $ db	Straight Line approx. dbs	error dbs
0.01	0.5	0	0	0
0.1	5.7	0.3	0	0.3
0.5	26.6	1.0	0	1.0
0.76	37.4	2.0	0	2.0
1.0	45.0	3.0	0	3.0
1.31	52.7	4.3	2.3	2.0
1.73	60.0	6.0	4.8	1.2
2.0	63.4	7.0	6.0	1.0
5.0	78.7	14.2	13.8	0.4
10.0	84.3	20.3	20	0.3

From this table it will be seen that the maximum error of 3 db occurs at the break frequency.

APPENDIX B



If we assume 100% efficiency, then the torque developed by the motor equals the torque necessary to drive the shaft, i.e.

$$kt V = J_m \ddot{\theta}_0 + F \dot{\theta}_0$$

where

kt = torque constant of the motor

J_m = moment of inertia of the shaft

F = viscous friction of motor

$\ddot{\theta}_0$ = angular acceleration

$\dot{\theta}_0$ = angular velocity

Taking the Laplace transform on both sides of the equation -

$$\begin{aligned} kt V (s) &= J_m S^2 \theta_0 + Fs \theta_0 \\ &= S (J_m S + F) \theta_0 \end{aligned}$$

or

$$\frac{\theta_0}{v} (s) = \frac{kt/F}{S(1 + J/F S)}$$

i.e.

$$\frac{\text{Motor shaft displacement}}{\text{control phase voltage}} \frac{\theta_0}{v} = \frac{K_m}{S(1 + T_m S)}$$

where

$$K_m = \frac{kt}{F} = \text{motor gain constant}$$

$$T_m = J/F = \text{motor time constant}$$

Dynamic Constant of Servo Motor

Rotor inertia J_m = $133 \cdot 10^{-6}$ gm-cm-sec² Control volts $V = 26v$

Stall Torque T_0 = 14.4 gm-cms

No Load speed N_0 = 6200 r.p.m.

Viscous friction $F = \frac{1}{2} \frac{\text{Stall Torque}}{\text{No load speed}} = \frac{T_0}{N_0} = 11.5 \times 10^{-3}$ gm-cms/rad/sec

Torque Constant $kt = \frac{\text{Stall Torque}}{\text{Control Volts}} = \frac{T_0}{V} = 0.55$ gm-cms/volt

$$\text{Motor Gain Constant } K_m = \frac{kt}{F} = \frac{0.55}{11.5 \times 10^{-3}} = 49/\text{V-sec}$$

$$\text{Motor Time Constant } T = J_m/F = \frac{133 \cdot 10^{-6}}{11.5 \times 10^{-3}} = 0.012 \text{ secs}$$

The motor transfer function is therefore -

$$\frac{\theta_o}{V}(s) = \frac{49}{s(1 + 0.012s)}$$

The Laplace operator S under steady state conditions can be replaced by jw . Thus the sinusoidal transfer function of the motor is -

$$\frac{\theta_o}{V} jw = \frac{49}{jw(1 + jw \cdot 0.012)}$$

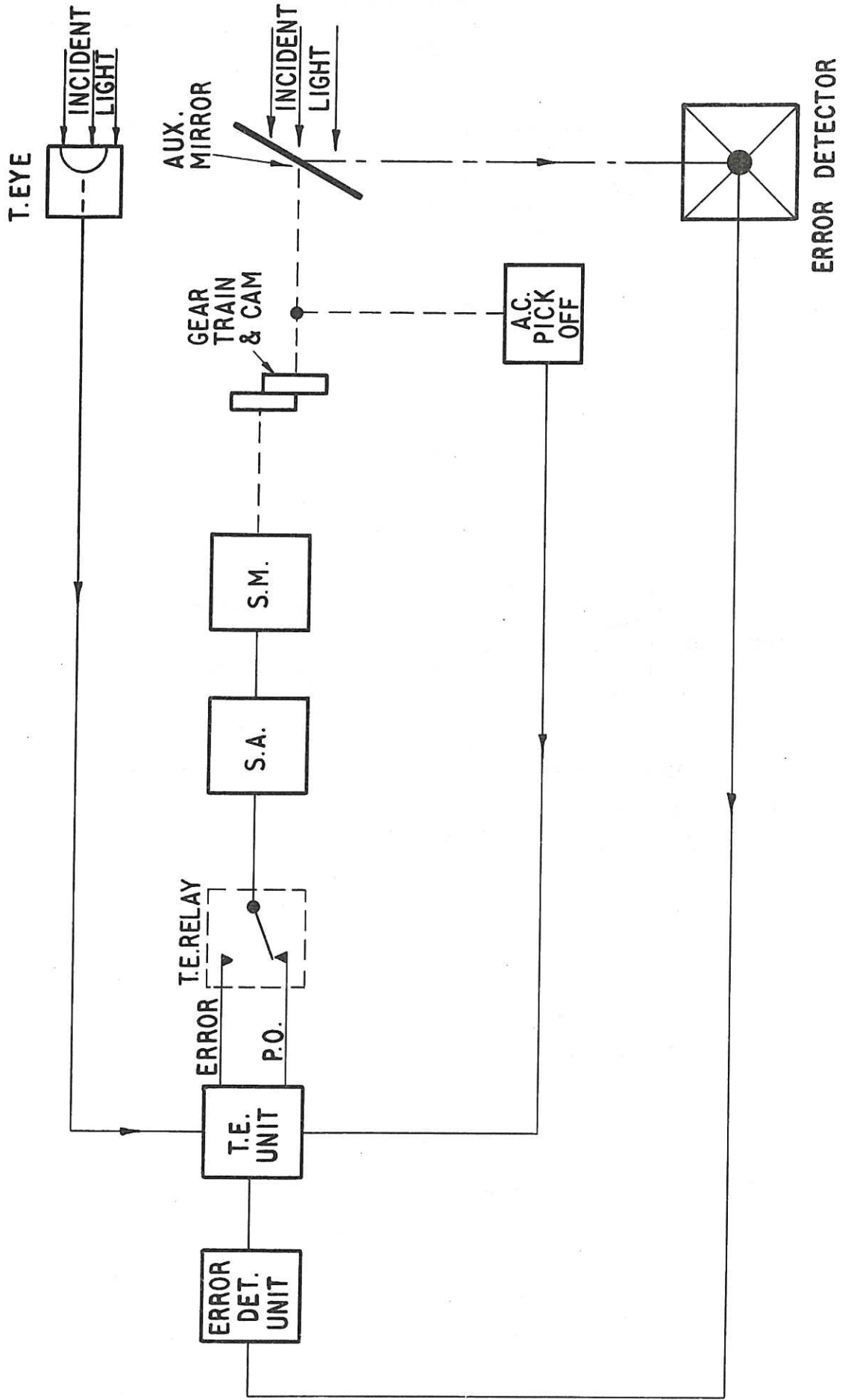


FIG. I. ONE AXIS OF SERVO - SYSTEM

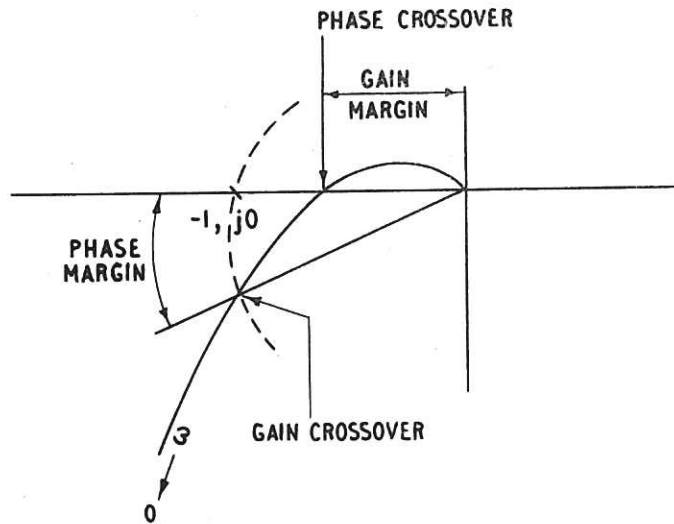


FIG. 2 NYQUIST PLOT

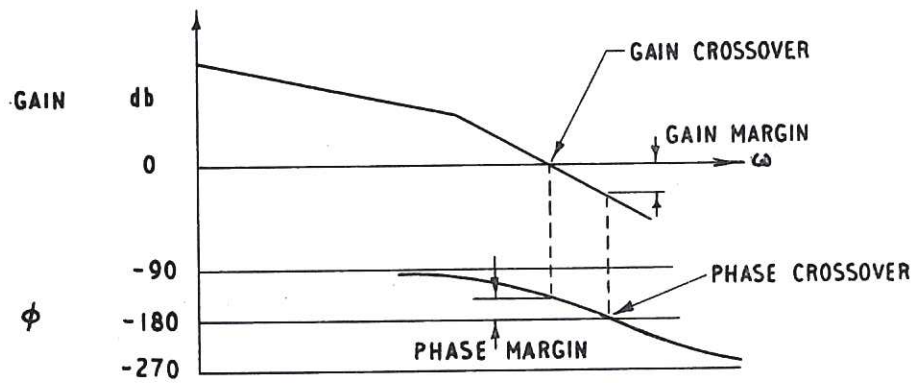


FIG. 3 BODE PLOT

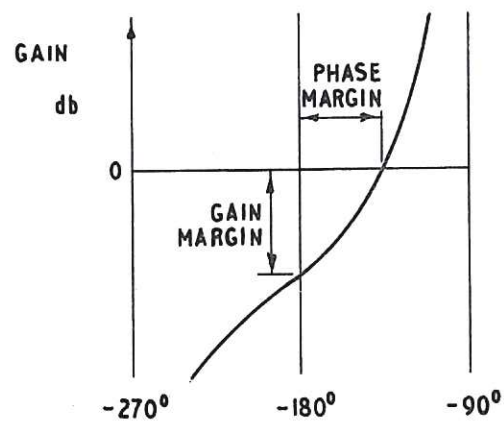
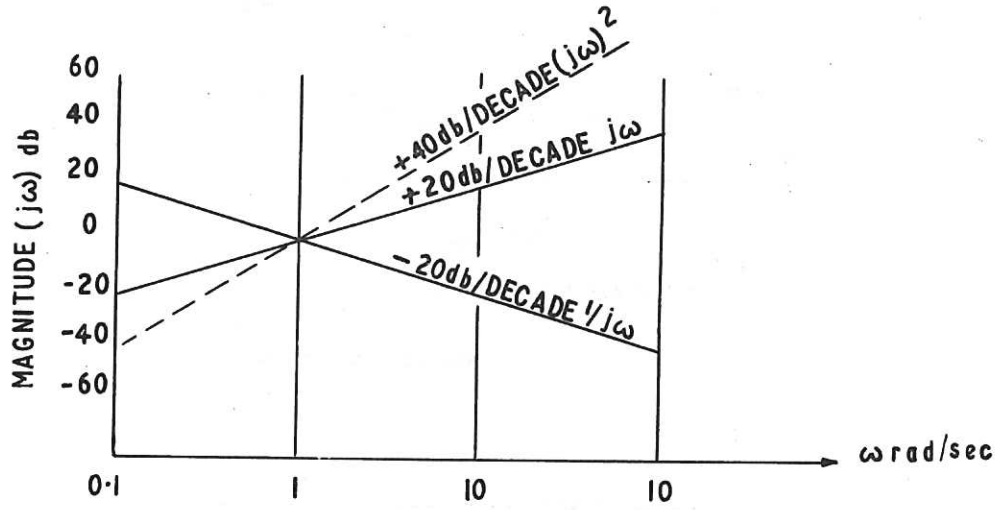


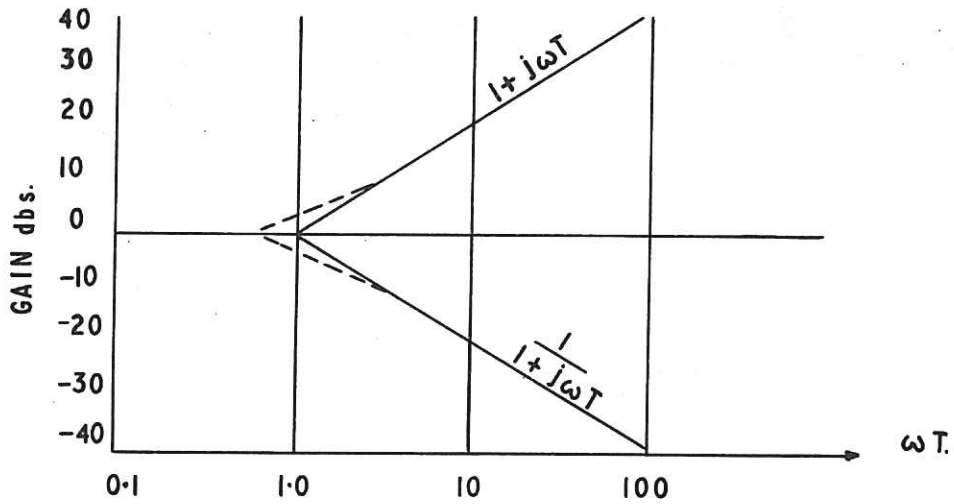
FIG. 4 GAIN PHASE PLOT

BODE PLOTS



PLOT OF $(j\omega)^{\pm n}$ $n=1, 2, \text{ ETC.}$

FIG. 5



PLOTS OF $(1+j\omega T)^{\pm 1}$

FIG. 6

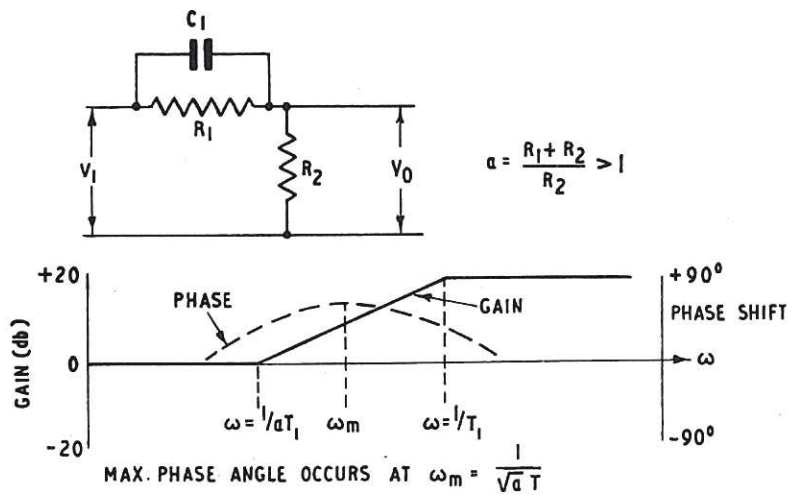


FIG.7 PHASE ADVANCE NETWORK

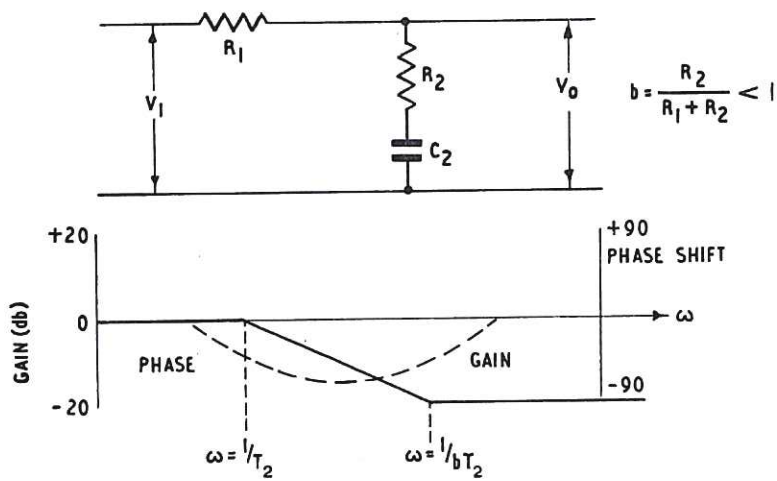


FIG.8 PHASE LAG NETWORK

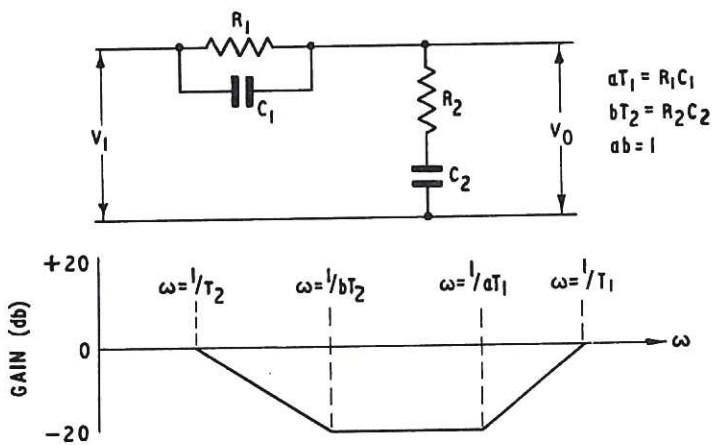


FIG.9 LEAD-LAG NETWORK

MOTOR CHARACTERISTICS

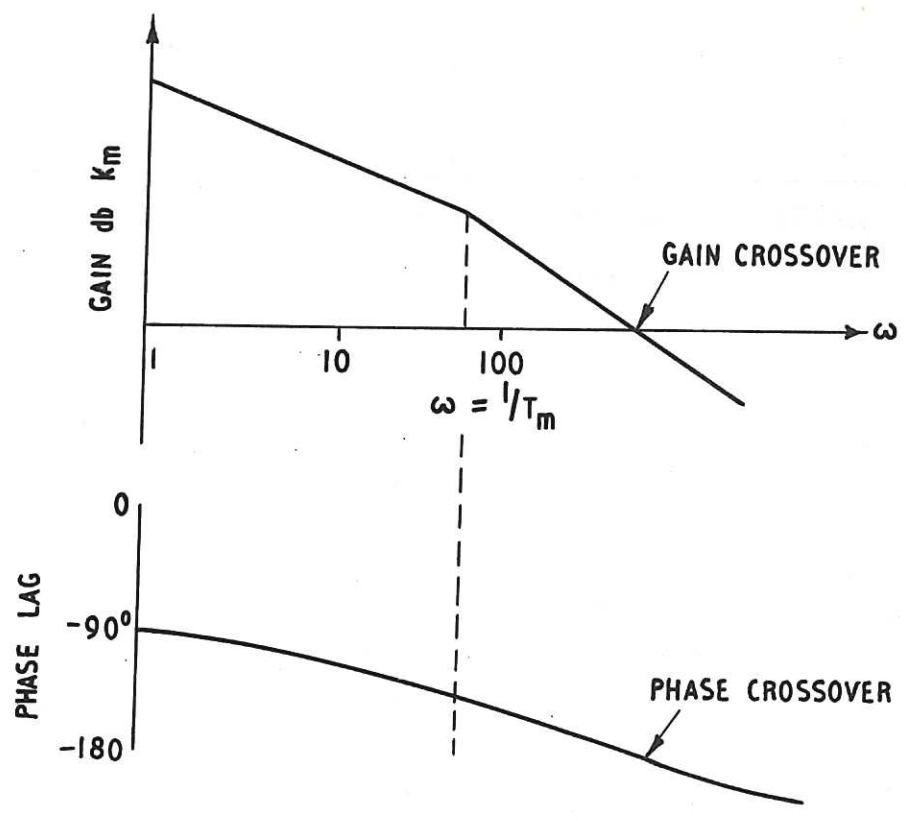
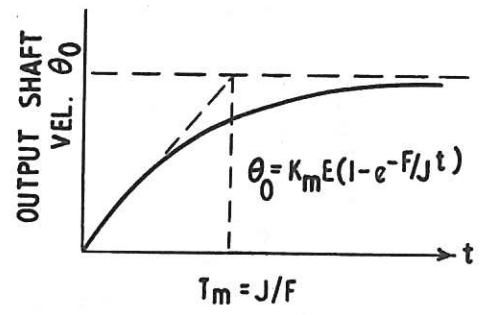
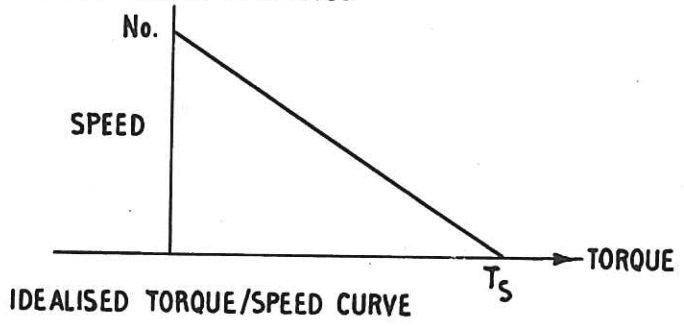


FIG. 10

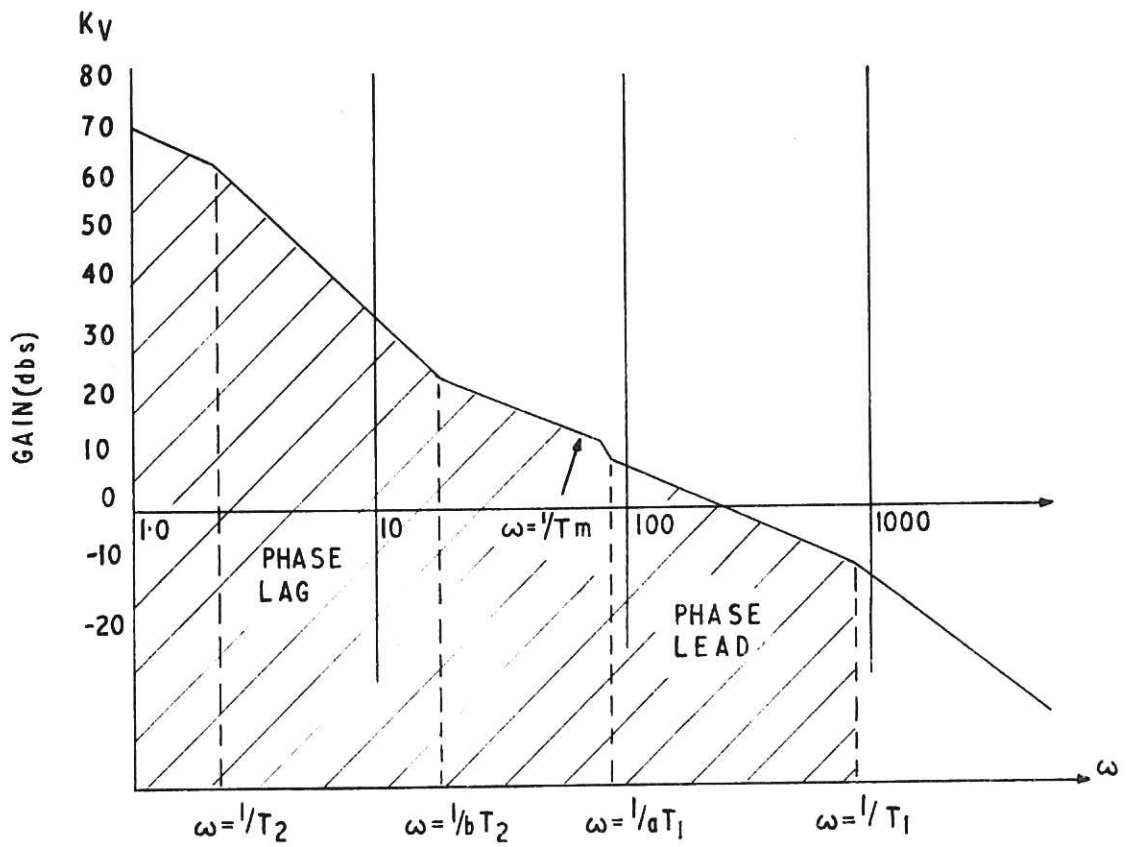


FIG. 11

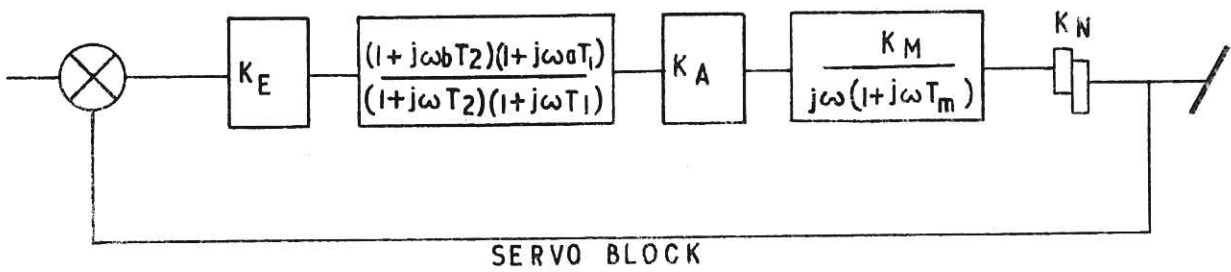


FIG. 12

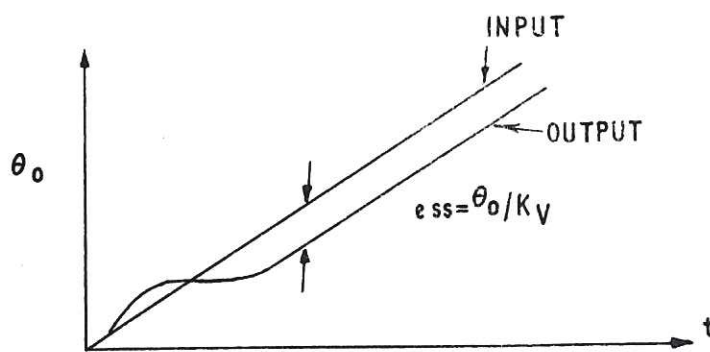


FIG. 13